



INDUCED ONE-PARAMETER BIFURCATIONS IN IDENTIFIED NONLINEAR DYNAMICAL MODELS

LUIS A. AGUIRRE

*Laboratório de Modelagem, Análise e Controle de Sistemas Não Lineares,
Departamento de Engenharia Eletrônica,
Universidade Federal de Minas Gerais,
Av. Antônio Carlos 6627, 31270-901 Belo Horizonte, Brazil*

JEAN MAQUET and CHRISTOPHE LETELLIER

*Groupe d'Analyse TOpologique et de MOdélisation de SYstèmes Dynamiques,
CORIA UMR 6614 – Université et INSA de Rouen,
Place Emile Blondel, F-76821 Mont Saint-Aignan Cedex, France*

Received February 8, 2001; Revised April 9, 2001

It is shown that nonlinear global models identified from a single time series can be used to reproduce the same sequence of bifurcations of the original system. This has been observed for simulated and real data and for both difference equation and differential equation models, thus suggesting some generality. The results reported in this paper are of a practical character and seem to have some bearing not only on the important subject of estimating bifurcation diagrams from data, but also in model validation problems since some models can reproduce the bifurcation sequence of a system even when such models do not settle to the original attractor at first. In this case, models which would be dismissed are shown to display consistent dynamic information about the original system, as illustrated by a simulated and a real data example. An additional example that uses real data is provided in which the original bifurcation sequence is recovered by the addition of multiplicative noise with increasing variance.

1. Introduction

The growing interest for nonlinear systems has motivated the development of techniques for nonlinear mathematical model building. To this end there are several representations from which to choose [Aguirre, 2000]. Broadly speaking, most techniques can be classified into two large groups, namely those that result in discrete-time models and those that result in continuous-time models. Nonlinear autoregressive moving average models with exogenous inputs (NARMAX) are an example of the former type [Leontaritis & Billings, 1985], whereas a set of differential equations is a typical example of the latter [Goesbet & Letellier, 1994]. These two representations will be considered in this paper.

A related problem that has been addressed recently is that of reconstructing bifurcation diagrams from data [Rico-Martinez *et al.*, 1992; Le Sceller *et al.*, 1996; Bagarinao *et al.*, 1999]. The objective is to obtain a mathematical model that produces a qualitatively similar bifurcation diagram to that of the system from which the data were obtained. Bagarinao and co-workers have derived a systematic two-step procedure for this [Bagarinao *et al.*, 1999]. First they assume K time series are measured at different parameter values of a dynamical system and fit K nonlinear models, with the same structure, to such data. In the second step, they parameterize the region occupied by the K parameter vectors using principal component analysis (PCA)

taking only the significant components. In this way they relate the model parameters (usually many) to a few (active) bifurcation parameters.

The main objective of this paper is to report that bifurcation diagrams that are qualitatively similar to that of the original system can be obtained from models identified from a single time series by varying one of the model parameters. Such results are interesting in several ways. First, it is shown that in many cases the bifurcation sequence of the original system can be retrieved using a model obtained from a *single* time series. Second, such a bifurcation sequence can be obtained by directly varying one of the model parameters without requiring any further parametrization. In this respect, however, a practical difficulty arises, namely the selection of a model parameter to be varied as a bifurcation parameter. Guidelines to aid in this choice in the case of continuous-time and discrete-time models are provided and illustrated with simulated and real data. Also, the results presented in this paper are especially relevant in global model validation problems, as will be argued.

In the investigation of the aforementioned problem, models derived for simulated and real nonlinear systems are analyzed. In order to have an impression of how general the observed scenario is, two very different modeling techniques were used. Such are briefly reviewed in Sec. 2. Section 3 presents the numerical examples. Section 4 discusses the main points of the paper and in the Appendix a real data example is provided in which the original bifurcation sequence is recovered by the addition of multiplicative noise with increasing variance.

2. Two Modeling Techniques

Consider a continuous-time dynamical system described by a set of ordinary differential equations

$$\dot{\mathbf{x}} = \mathbf{f}(\mathbf{x}; \boldsymbol{\mu}), \quad (1)$$

where $\mathbf{x}(t) \in \mathbb{R}^n$ is the state vector that depends on a parameter t called the time and \mathbf{f} , the so-called vector field, is an n -component smooth function generating a flow ϕ_t . Also, $\boldsymbol{\mu} \in \mathbb{R}^p$ is the parameter vector with p components, assumed to be constant in this work.

It is assumed that a single variable is measured, and it is desired to obtain a dynamical model, from that single time series and with no prior knowledge, that will represent the original dynamics in some

sense. In the remainder of this session, two different model representations will be described. Such representations will be used on simulated and real data to illustrate the main ideas of this work.

2.1. Discrete-time polynomials

Here it is considered that the measured time series is $y(k) = h(\mathbf{x}(kT_s))$, $k = 0, 1, \dots$ and where T_s is the sampling time. In many cases, the time evolution of the observed $y(k)$ can be described by a nonlinear autoregressive moving average (NARMA) model [Leontaritis & Billings, 1985] of the form

$$y(k) = F^\ell[y(k-1), \dots, y(k-n_y), e(k), \dots, e(k-n_e)], \quad (2)$$

where n_y and n_e are the maximum lags considered for the process and noise terms, respectively. Moreover, $y(k)$ is the output time series and $e(k)$ accounts for uncertainties, possible noise, unmodeled dynamics. $F^\ell[\cdot]$ is some nonlinear function of $y(k)$ and $e(k)$.

In this paper, the map $F^\ell[\cdot]$ is a polynomial of degree $\ell \in \mathbb{Z}^+$. In order to estimate the parameters of this map, Eq. (2) can be expressed as:

$$y(k) = \boldsymbol{\psi}(k-1)^T \hat{\boldsymbol{\theta}} + \xi(k), \quad (3)$$

where $\xi(k)$ are the identification residuals. Moreover, $\boldsymbol{\psi}(k-1)$ is a vector which contains output and residual terms up to and including time $k-1$, and $\hat{\boldsymbol{\theta}}$ is the estimated parameter vector obtained by minimizing the following cost function [Chen *et al.*, 1989]:

$$J_N(\hat{\boldsymbol{\theta}}) = \frac{1}{N} \sum_{k=1}^N \xi^2(k, \hat{\boldsymbol{\theta}}). \quad (4)$$

The variance of the parameter vector estimated by least squares is:

$$\text{var}(\hat{\boldsymbol{\theta}}_{\text{LS}}) = \sigma_e^2 [\boldsymbol{\Psi}^T \boldsymbol{\Psi}]^{-1}, \quad (5)$$

where σ_e^2 is the variance of the white noise that corrupts the data and $\boldsymbol{\Psi}$ is the regressor matrix obtained by taking $\boldsymbol{\psi}(k-1)^T$ over the data records. In practice, σ_e^2 is approximated by the variance of the residuals $\xi(k)$. As can be seen in Eq. (5), the variance of any least squares estimate will be inversely proportional to the signal/noise ratio of the data.

Parameter estimation is usually performed for a linear-in-the-parameters orthogonal model which is closely related to (3) and which is represented as:

$$y(k) = \sum_{i=1}^{n_p+n_\xi} g_i w_i(k) + \xi(k), \quad (6)$$

where $n_p + n_\xi$ is the number of (process plus noise) terms in the model, $\{g_i\}_{i=1}^{n_p+n_\xi}$ are parameters and the monomials $\{w_i(k)\}_{i=1}^{n_p+n_\xi}$ are orthogonal over the data records. Finally, parameters of the model in Eq. (3) can be calculated from the $\{g_i\}_{i=1}^{n_p+n_\xi}$. This procedure has two major advantages, viz. (i) reduces inaccuracies due to numerical ill-conditioning; (ii) aids in selecting the structure of the final model.

A criterion for selecting the most important terms in the model can be devised as a by-product of the orthogonal parameter estimation procedure. The reduction in the mean square prediction error (MSPE) due to the inclusion of the i th term, $g_i w_i(k)$, in the auxiliary model of Eq. (6) is $(1/N)g_i^2 \overline{w_i^2(k)}$. Expressing this reduction in terms of the total MSPE yields the error reduction ratio (ERR):

$$[\text{ERR}]_i \doteq \frac{g_i^2 \overline{w_i^2(k)}}{y^2(k)}, \quad i = 1, 2, \dots, n_p + n_\xi. \quad (7)$$

Hence those terms with large values of ERR are selected to form the model.

2.2. Continuous-time polynomials

In this approach it is assumed that a single scalar time series, $X_1 = x = h(\mathbf{x})$, is recorded, where, as before, $h(\cdot)$ is a measurement function. The aim is then to obtain a vector field equivalent to the original system using a basis consisting of the observable and its derivatives such as

$$\dot{X}_1 = X_2; \quad \dot{X}_2 = X_3; \quad \dots \quad \dot{X}_{d_e} = F(X_1, X_2, \dots, X_{d_e}), \quad (8)$$

where d_e is the embedding dimension and F depends on d_e variables which are x and the $d_e - 1$ successive derivatives of x . F can be estimated by using a multivariate polynomial basis on nets [Gouesbet & Letellier, 1994]. The algorithm requires the definition of modeling parameters which are:

1. d_e , the embedding dimension,

2. N_c , the number of centers at which the function is evaluated,
3. Δt , the time step between two successive centers. In this work Δt is constant, but this is not a requirement,
4. N_p , the number of retained multinomials, and
5. τ_w , the window length on which the derivatives are computed by using polynomial interpolation over the window.

Derivatives are then obtained by analytically derivating such polynomials. The estimated function, \hat{F} , then reads as

$$\hat{F}(X_1, X_2, \dots, X_{d_e}) = \sum_{p=1}^{N_p} \theta_p \psi^p, \quad (9)$$

where θ_p are the parameters and ψ^p are multivariate monomials (or multinomials) of the form

$$\psi^p = X_1^{n_1} X_2^{n_2} \dots X_{d_e}^{n_{d_e}}, \quad (10)$$

where the integers p are related to n_{d_e} -uplets $(n_1, n_2, \dots, n_{d_e})$ by a bijective relationship discussed in [Gouesbet & Letellier, 1994]. The modeling parameters d_e , N_c , Δt , N_p and τ_w can be determined with the aid of an error function described in [Le Sceller *et al.*, 1996]. The model (9) is based on a differential embedding.

Writing (9) at N_c centers on the data yields a set of N_c equations of the form

$$\begin{bmatrix} \dot{X}_{d_e}(1) \\ \vdots \\ \dot{X}_{d_e}(N_c) \end{bmatrix} = \begin{bmatrix} \psi^{r_1}(1) & \dots & \psi^{r_{n_p}}(1) \\ \vdots & & \vdots \\ \psi^{r_1}(N_c) & \dots & \psi^{r_{n_p}}(N_c) \end{bmatrix} \begin{bmatrix} \theta_{r_1} \\ \vdots \\ \theta_{r_{n_p}} \end{bmatrix}, \quad (11)$$

where $r_i \neq r_j$ and $1 \leq r_1 \dots r_{n_p} \leq N_p$ and the numbers inside the parentheses indicate to which center the variable is related. Once the model structure is determined the parameter vector $[\hat{\theta}_{r_1} \dots \hat{\theta}_{r_{n_p}}]^T$ can be estimated by standard least squares techniques.

3. Bifurcations of Identified Models

This section presents a couple of examples in which identified models are used to produce a bifurcation sequence equivalent to that of the original systems.

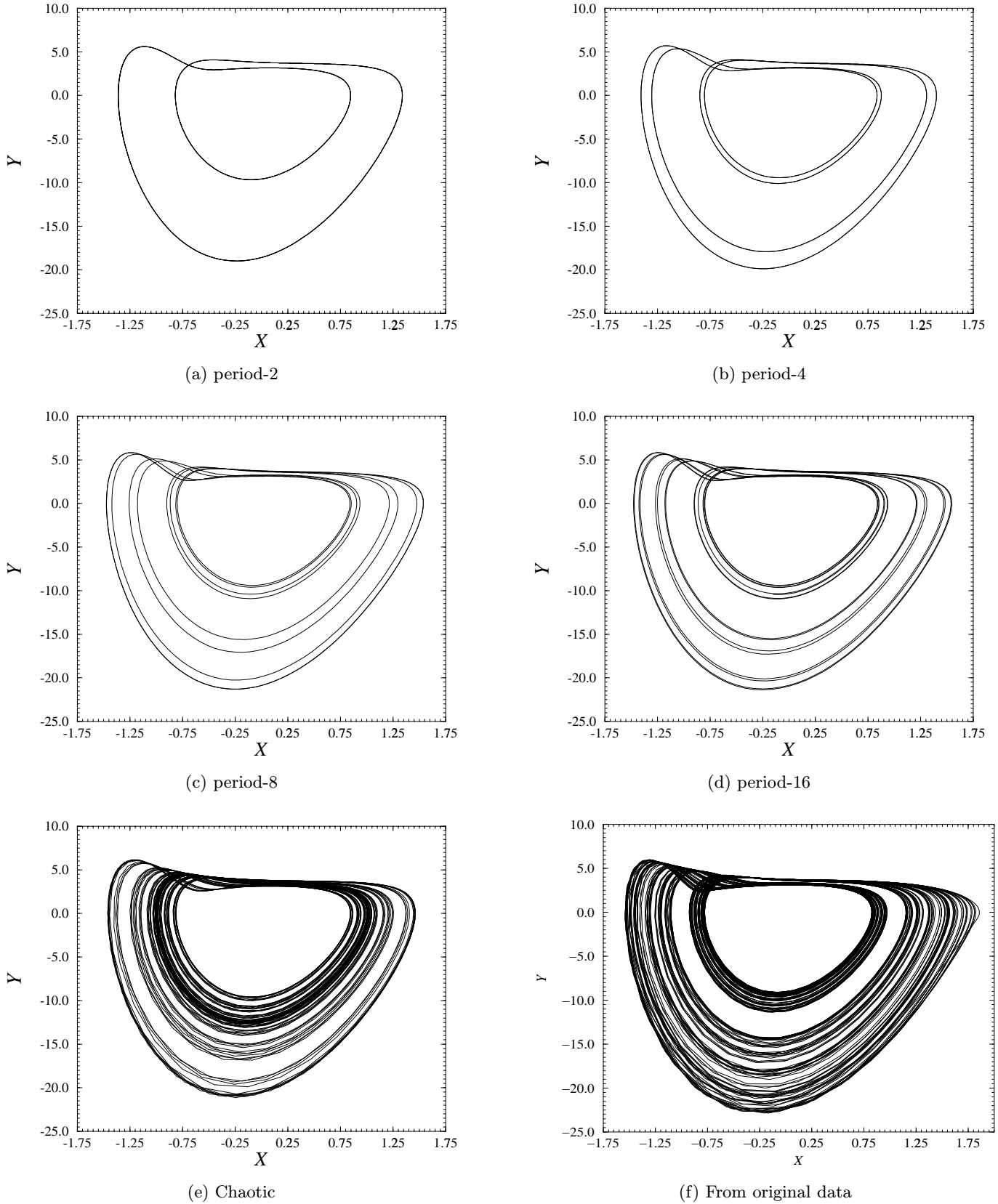


Fig. 1. (a–e) are attractors produced by a perturbed model obtained using $(N_c, N_{pp}, N_p) = (57, 8, 20)$ and setting $\theta_{19} = \theta_{20} = 0.0$. The period-doubling cascade observed when the coefficient θ_{11} is increased is analogous to the period-doubling cascade of the original Burke'n Shaw system. (a) $\theta_{11} = 80$, (b) $\theta_{11} = 100$, (c) $\theta_{11} = 135$, (d) $\theta_{11} = 136$, (e) $\theta_{11} = 151$ (notice that scale is slightly different), (f) attractor reconstructed from data.

3.1. The Burke'n Shaw system

Consider the Burke'n Shaw system

$$\begin{cases} \dot{x} = -S(y + x) \\ \dot{y} = -Sxz - y \\ \dot{z} = S y x + V, \end{cases} \quad (12)$$

with $(S, V) = (10.0, 3.811)$ which generates a chaotic behavior as seen in Fig. 1(f). The integration step was $\delta t = 2 \times 10^{-3}$ s. The following modeling parameters were used in this example: degree of nonlinearity equal to 3, number of terms $N_p = 20$, embedding dimension $d_e = 3$, time step between two successive centers $\Delta t = 16 \times 10^{-3}$ (corresponding to $N_{pp} = 8$) and N_c between 55 and 60. Only limit cycles as shown in Fig. 1(b) were obtained from the estimated models.

During the search for models, most coefficients θ_p significantly change when N_c is increased. But it has been noted that θ_{19} and θ_{20} are always very small. These parameters happen to be irrelevant and can be deleted. On the other hand,

θ_{11} , the parameter of X^3 , remains almost constant (see Table 1). The consistency of θ_{11} is an indication that such a parameter (and the corresponding term X^3 also) is somewhat fundamental in the model. This motivates the choice of θ_{11} as a parameter to be changed in order to perturb the model. In fact, varying θ_{11} induces the bifurcation sequence shown in Fig. 1. In particular, for $\theta_{11} = 80$ [Fig. 1(a)] a period-2 limit cycle is obtained, for $\theta_{11} = 100$ [Fig. 1(b)] a period-4, for $\theta_{11} = 135$ [Fig. 1(c)] a period-8 and, finally, for $\theta_{11} = 141$ [Fig. 1(d)] a period-16. This parameter controls a period-doubling bifurcation cascade leading to chaos [Fig. 1(e)] for $\theta = 151$. The model diverges when θ_{11} is increased beyond 151.50. It is noted that perturbations in other parameters resulted in unstable models.

This example started with data taken from the chaotic attractor shown in Fig. 1(f). After a systematic search for models, the best model generated the period-four limit cycle similar to the one shown in Fig. 1(b). Of course, this attractor is quite

Table 1. Coefficients of the models for two different values of N_c . Most coefficients significantly change except θ_{11} which is almost constant. Also remark that the last two coefficients have very small values. These coefficients were deleted from the perturbed model in which θ_{11} was used as a bifurcation parameter.

p	θ_p		
	$(N_c, N_{pp}, N_p) = (57, 8, 20)$	$(N_c, N_{pp}, N_p) = (58, 8, 20)$	(n_1, n_2, n_3)
1	98.326134176008	103.02285047560	0 0 0
2	-1427.9409152157	-1443.6166825827	1 0 0
3	-56.181408873324	-56.844200088367	0 1 0
4	-22.232022492197	-22.372048961485	0 0 1
5	501.52403460705	467.71075686050	2 0 0
6	403.57658006053	407.96604131899	1 1 0
7	7.4584153697660	7.4123180422492	1 0 1
8	6.5153053496969	6.3478895134472	0 2 0
9	0.13604832401699	0.16301652021131	0 1 1
10	-0.049159391759640	-0.042693351871938	0 0 2
11	104.70788950540	104.03675580967	3 0 0
12	-180.48678800329	-171.04092181341	2 1 0
13	6.4361846245595	5.7076855194178	2 0 1
14	-0.72664566763736	-0.75847675787585	1 2 0
15	0.34761225763095	0.28768076093647	1 1 1
16	0.0062514963734994	0.0045001659682714	1 0 2
17	0.092721813118938	0.089834581471049	0 3 0
18	-0.013480909352725	-0.010757271661776	0 2 1
19	0.00046360740432311	0.00037352780786374	0 1 2
20	0.000014680824758598	0.000011320664942690	0 0 3

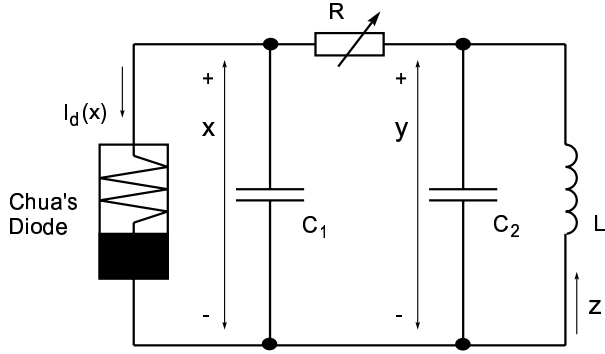


Fig. 2. Chua's circuit.

different from the original one and the model shown in Table 1 could be easily dismissed as invalid. However, a perturbation of this model produces a chaotic attractor that is quite close to the original one, as can be seen in Fig. 1(e). In addition to that, varying a parameter results in a period-doubling cascade to chaos, just like for the original system when parameter V is varied. In the present example, the parameter to vary was chosen as the one with greatest consistency, in the sense that such a parameter is less sensitive to variations in the modeling parameter N_c . Finally, it should be pointed out that in the present example the estimated value of θ_{11} had to be varied around 50% in order to get a chaotic attractor close to the original one. The next example considers a case in which the variations are quite small (around 3%) and variations within plus and minus one standard deviation of the estimated parameter suffice to reproduce the entire bifurcation sequence.

A quite surprising example is presented in the Appendix. A continuous-time model estimated from a single time series recorded from copper electro-dissolution in phosphoric acid [Letellier *et al.*, 1995a] has been perturbed with multipli-

cative noise. The variance of this noise can be taken as a bifurcation parameter which allows to reproduce the bifurcation diagram observed in the experiments.

3.2. Chua's circuit

An identification data set on the double scroll attractor of Chua's circuit, shown in Fig. 2 [Chua & Hasler, 1993], was measured using an 8-bit A/D converter with sampling time $T_s = 12 \mu\text{s}$. The signal/noise ratio ($\text{SNR} = 20 \log(\sigma_y^2/\sigma_e^2)$) estimated from these data was 47.51 dB. The relatively low resolution used generated high digitalization errors which appear as additive noise to the identification algorithms. Low signal/noise ratios hamper both model structure selection and parameter estimation. In fact, the ERR criterion does select inadequate structures from noisy data but this mismatch can be avoided using cluster analysis [Aguirre *et al.*, 1997]. Besides, as seen in Sec. 2.1, the variance of model parameters depends directly on the variance of the noise that corrupts the identification data.

It is desired to investigate the bifurcation sequence presented by a NARMA model identified from real data on the double scroll attractor. In the first stage, the focus will be the bifurcations caused by variations in the model parameter of the linear term with highest ERR, \hat{a}_1 . In the second stage, the model bifurcations are induced by variations in the parameter which multiplies the cubic term with highest ERR, \hat{a}_3 . The motivation for varying such parameters comes from the definition of the ERR criterion. According to ERR, such parameters correspond to the most important linear and cubic terms, respectively.

Consider the monovariate NARMA model which was identified from data on the double scroll attractor. The model terms appear in decreasing values of ERR

$$\begin{aligned}
 y(k) = & 1.3902y(k-1) - 0.6483y(k-4) - 1891.2489y(k-1)y(k-5)y(k-6) \\
 & + 4628.2549y(k-2)y(k-4)y(k-6) + 0.6199y(k-6) + 0.3634y(k-2) \\
 & - 0.2903y(k-3) - 2415.2616y(k-3)y(k-4)y(k-5) - 0.3988y(k-5) \\
 & - 527.2104y(k-1)^3 - 2915.2755y(k-6)^3 + 6979.7872y(k-4)y(k-6)^2 \\
 & + 921.1841y(k-1)y(k-2)y(k-3) + 50.8122y(k-5)y(k-6)^2 \\
 & - 1932.6477y(k-2)^2y(k-6) - 4953.4587y(k-4)^2y(k-6) \\
 & - 1869.3976y(k-2)y(k-6)^2 + 2054.9849y(k-1)y(k-4)y(k-5) \\
 & + 2250.7216y(k-3)y(k-5)y(k-6) - 558.6647y(k-1)y(k-6)^2.
 \end{aligned} \tag{13}$$

Table 2. Dynamical regimes obtained varying model (13) parameters \hat{a}_1 and \hat{a}_3 one at a time. While varying one parameter the other one was fixed at the value shown in model (13). \tilde{a}_1 and \tilde{a}_3 indicate the specific values considered.

Dynamical Regime	\tilde{a}_1	\tilde{a}_3
Stable nontrivial fixed point	1.3662	-1.7936×10^3
Period one limit cycle	1.3902	-1.8912×10^3
Period two limit cycle	1.3972	-1.9303×10^3
Period four limit cycle	1.3992	-1.9390×10^3
Spiral attractor	1.4002	-1.9465×10^3
Period three limit cycle	1.4012	-1.9516×10^3
Spiral attractor	1.4022	-1.9693×10^3
Double scroll attractor	1.4092	-2.0263×10^3
Unstable dynamics	1.4322	-2.2063×10^3

The model terms were automatically selected using the ERR criterion from a set of 84 candidate terms formed by the union of all linear and cubic terms. The constant and the quadratic terms were previously excluded based on cluster and high-order spectral analysis [Aguirre *et al.*, 1997; Aguirre, 1997].

The least squares estimate of \hat{a}_1 (parameter of the term $y(k-1)$) is $\hat{a}_1 = 1.3902 \pm 0.0540$. Hence, considering a Gaussian distribution for the estimates, there is 68% probability that the nominal parameter will be in the interval $1.3362 \leq \tilde{a}_1 \leq 1.4442$ (assuming that the residuals are white). The variation of \hat{a}_1 within the cited interval generated the new dynamical behaviors summarized in Table 2. Such a table shows that it is possible to generate a model with chaotic dynamics via the perturbation of \hat{a}_1 within its estimation confidence interval. Therefore, the identified structure is able to reproduce the desired dynamics. An exceeding perturbation in parameter \hat{a}_1 results in unstable models. Figure 3(c) shows the chaotic attractor reconstructed with $\tilde{a}_1 = 1.4092$. Hence all it takes for the identified model to reproduce the original bifurcation sequence is a small perturbation in just

one parameter (out of twenty). It is further stressed that this information is somewhat coded into a single time series obtained from the real circuit operating with *fixed* parameters and there is no need, at least in principle, to consider a large set of time series at different parameter values.

As mentioned earlier, parameter \hat{a}_3 of model (13) (parameter which corresponds to term $y(k-1)y(k-5)y(k-6)$) also induces a similar bifurcation sequence, although the double scroll attractor obtained in this way is visibly smaller than the original one. This should come as no surprise since it is known that varying different model parameters can induce very similar bifurcation diagrams. Figure 3(d) shows the chaotic attractor reconstructed with $\tilde{a}_3 = -2.0263 \times 10^3$. The least squares estimate of this parameter is $\hat{a}_3 = -1.8912 \times 10^3 \pm 9.7600 \times 10^2$. The parameter variation within the range $-2.8672 \times 10^3 \leq \tilde{a}_3 \leq -9.1520 \times 10^2$ generated new dynamical regimes which are presented in Table 2 thus confirming that the same bifurcation sequence of the original circuit is recovered.

It is worth pointing out that perturbations in other parameters of (13) resulted in unstable models, as for the continuous-time models. Thus, it seems that the ERR indicates the more suitable parameters to be varied, for the discrete-time models.

Table 3 presents the fixed points and estimates of the correlation dimension, d_c , and of the largest Lyapunov exponent, λ_1 , for some model attractors. In the case of fixed-points, only the inductor current component is shown. The correlation dimension and the largest Lyapunov exponent were estimated using the MTRCHAOS software [Rosenstein, 1993].

As seen in Tables 2 and 3, the identified model (13) can be used to reproduce the same sequence of one-parameter bifurcations as the original circuit. Moreover, the attractors thus obtained reproduce the circuit dynamical properties to some extent. This confirms that the structure of model

Table 3. Fixed points and dynamical invariants of some modified models.

Model	Fixed Point	D_c	λ_1
Chua's circuit	(-12.30, 0, 12.30) mA	2.06	0.029
Model (13)	(-14.27, 0, 14.27) mA	1	< 0
Chaotic model $\tilde{a}_1 = 1.4092$	(-17.63, 0, 17.63) mA	1.96	0.025
Chaotic model $\tilde{a}_3 = -2.0263 \times 10^3$	(-10.75, 0, 10.75) mA	2.17	0.027

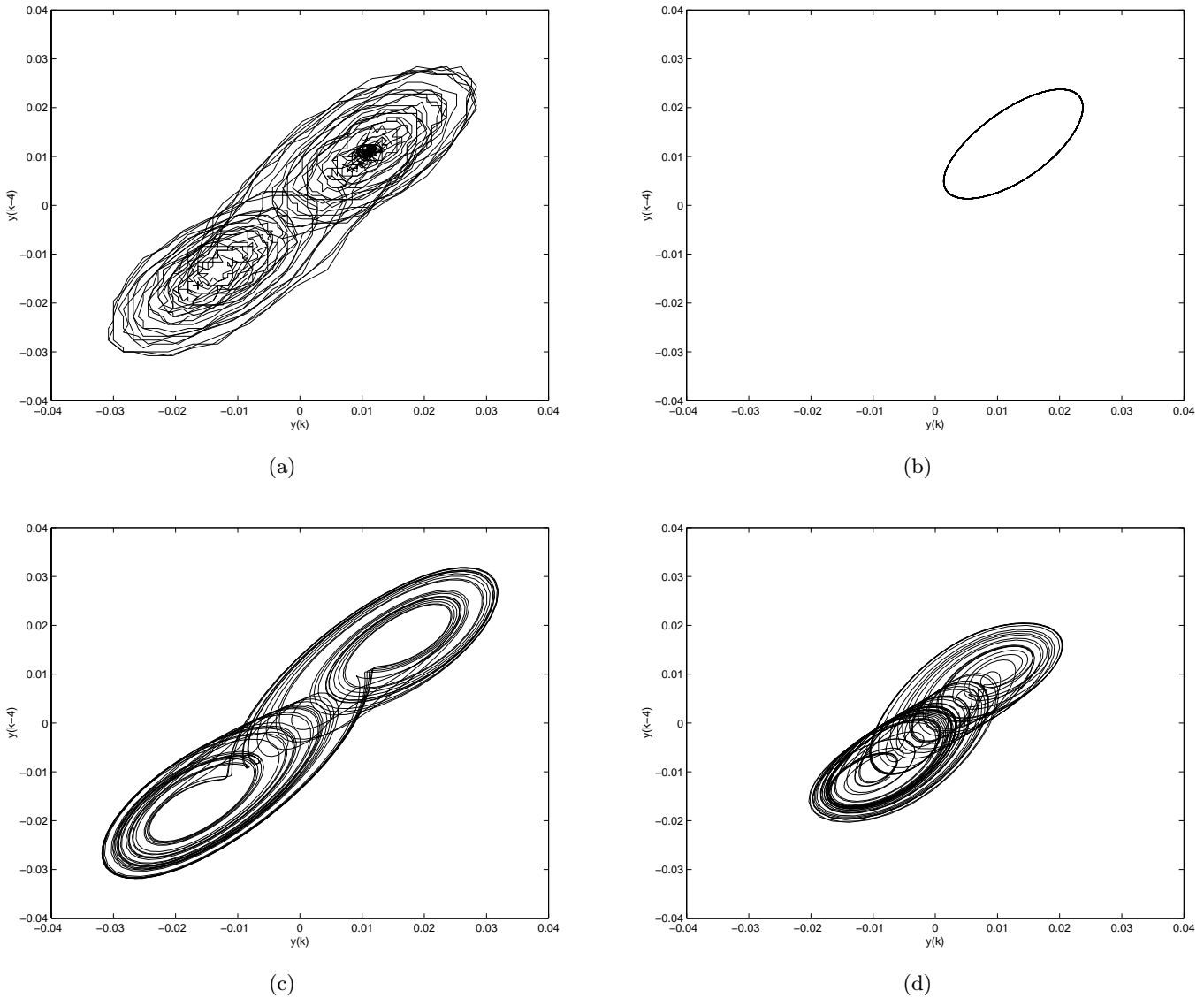


Fig. 3. Bidimensional projection of reconstructed attractors of Chua's circuit. (a) Identification data attractor. Note the low signal to noise ratio due to digitalization, (b) attractor of identified model (13), (c) attractor obtained for $\tilde{a}_1 = 1.4902$. (d) Model obtained through variation in $\tilde{a}_3 = -2.0263 \times 10^3$.

is adequate to represent the double scroll attractor although the original estimated parameters have fallen out of its attraction basin (see discussion in Sec. 4).

4. Discussion and Conclusion

It has been shown that identified models obtained from a single time series can be used to reproduce a bifurcation sequence that is equivalent to that of the original system by varying one of the model parameters. Hence, it is possible to reproduce dynamical regimes of the original system not directly apparent in the available time series. This scenario

has been observed in a great number of simulated and real data examples using different model representations. For the sake of space, this paper has reported two examples that involve simulated and real data with continuous-time and discrete-time model representations. This seems to support that the observed scenario is somewhat general. Further research is needed to better understand the phenomena involved.

It is believed that these conclusions are not only relevant in the important problem of reconstructing bifurcation diagrams from data [Le Sceller *et al.*, 1996; Bagarinao *et al.*, 1999] but also have a direct bearing on the understanding of nonlinear models and are useful in their validation.

It very often happens, when modeling nonlinear dynamics, the obtained model reproduces an attractor which is apparently very different from the original one. At first sight, the only reasonable thing to do is to reject the model during validation. However, in many instances it has been noticed that a model that at first does not reproduce the original attractor might have all the basic dynamical information required. Frequently, a perturbation of such a model will result in an attractor quite close to the original one. Moreover, frequently the bifurcation diagram of the model closely resembles that of the original system. This would point to the fact that in such cases the model that had been obtained was

in fact representative of the system and in such a case an attractor close to the original one can be achieved by perturbing the model.

If the model is considered as a point in parameter space, different regions of such a space correspond to different dynamical regimes displayed by the model with the respective parameters. Frequently an insignificant variation in one or more parameters can drastically change the dynamical behavior of the model. In many instances, the models fall outside the parameter region corresponding to the intended attractor as a consequence of noise or slightly nonoptimal modeling parameters such as the number of terms, embedding dimension

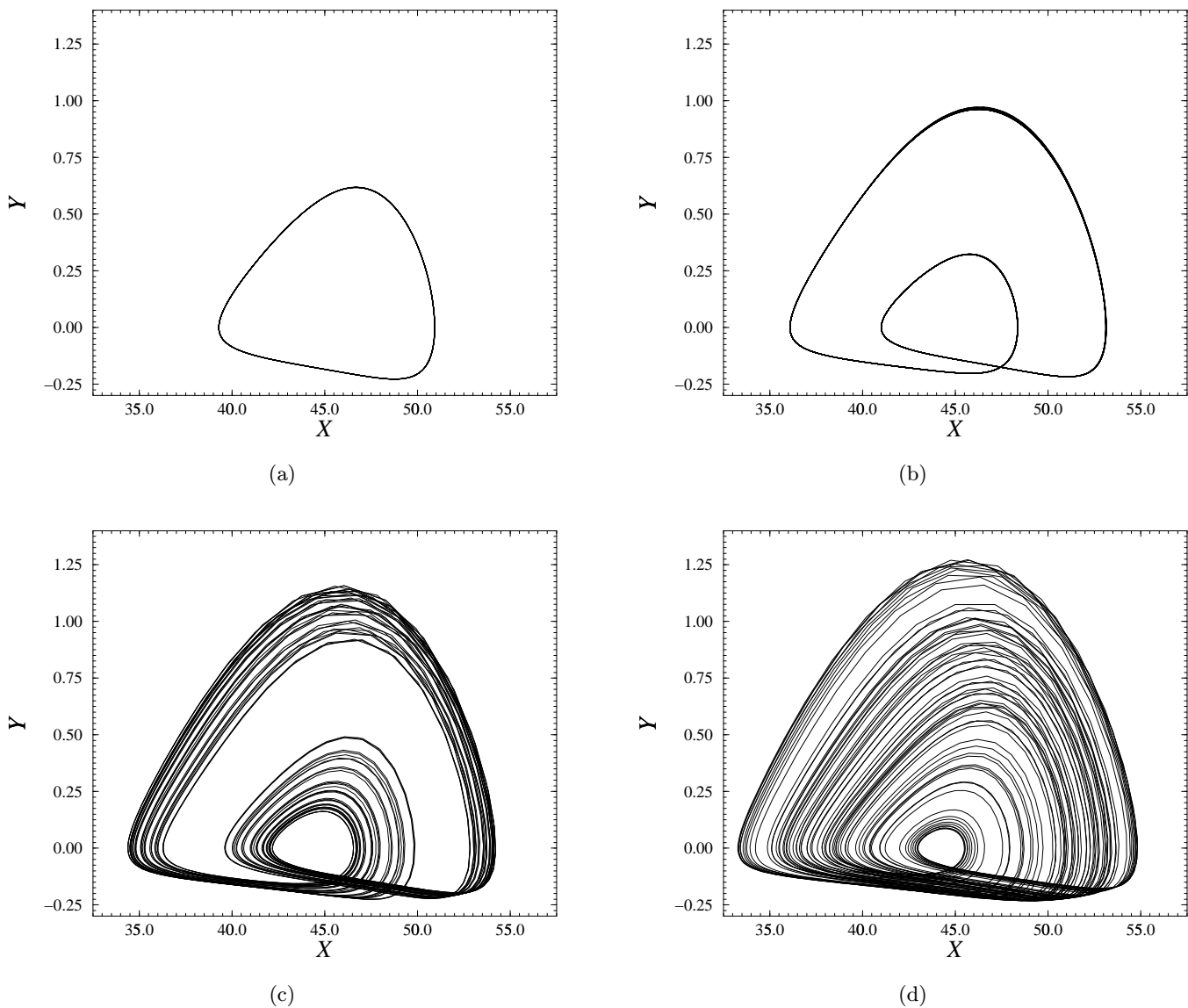


Fig. 4. Different typical attractors generated by the global continuous model obtained, starting from a single scalar time series with multiplicative noise.

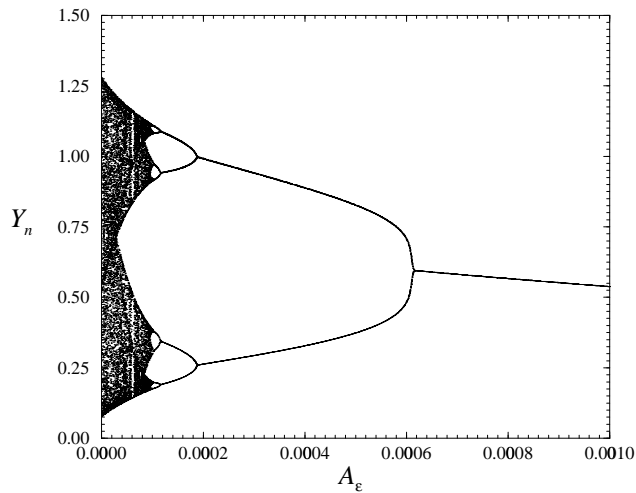


Fig. 5. Bifurcation diagram versus the amplitude of the multiplicative noise applied to the model.

and number of centers used [Letellier *et al.*, 1995b]. This is apparently the case in many instances reported in the literature which do not seem to be fully understood, e.g. Fig. 5 of [Chon *et al.*, 1997]. It is important to note that such models are outside but often in a vicinity of dynamically valid models. Therefore, a small perturbation in many cases is sufficient to shift the model back into the desired dynamical regime.

An open problem seems to be how to choose which parameter to vary in order to perturb the model when only one time series and respective model are available. In this paper simple and effective procedures have been suggested and illustrated for this purpose. Of course, many more can be devised. For instance, principal component analysis (PCA) can be used to define bifurcation parameters when a set of time series and models are available [Bagarinao *et al.*, 1999].

Acknowledgments

This work has been supported by CNPq and CNRS. It has recently been brought to our attention that a related investigation is being developed with similar objectives but starting from models obtained with some prior knowledge [Bezruchko *et al.*, 2001].

References

Aguirre, L. A. [1997] "On the structure of nonlinear polynomial models: Higher-order correlation functions, spectra and term clusters," *IEEE Trans. Circuits Syst. I* **44**(5), 450–453.

- Aguirre, L. A., Rodrigues, G. G. & Mendes, E. M. [1997] "Nonlinear identification and cluster analysis of chaotic attractors from a real implementation of Chua's circuit," *Int. J. Bifurcation and Chaos* **7**(6), 1411–1423.
- Aguirre, L. A. [2000] "A nonlinear dynamical approach to system identification," *IEEE Circuits Syst. Soc. Newslett.* **11**(2), 10–23, 47.
- Albahadily, F. & Schell, M. [1988] "An experimental investigation of periodic and chaotic electrochemical oscillations in the anodic dissolution of copper in phosphoric acid," *J. Chem. Phys.* **88**(7), 4312–4319.
- Bagarinao, E., Pakdaman, K., Nomura, T. & Sato, S. [1999] "Reconstructing bifurcation diagrams from noisy time series using nonlinear autoregressive models," *Phys. Rev.* **E60**(1), 1073–1076.
- Bezruchko, B. P., Seleznev, Y. P. & Smirnov, D. A. [2001] "On the possibility of constructing a bifurcation diagram from an experimental time series," submitted.
- Chen, S., Billings, S. A. & Luo, W. [1989] "Orthogonal least squares methods and their application to nonlinear system identification," *Int. J. Contr.* **50**(5), 1873–1896.
- Chon, K. H., Kanters, J. K., Cohen, R. J. & Holstein-Rathlou, N. H. [1997] "Detection of chaotic determinism in time series from randomly forced maps," *Physica* **D99**, 471–486.
- Chua, L. O. & Hasler, M. (guest eds.) [1993] Special issue on "Chaos in nonlinear electronic circuits," *IEEE Trans. Circuits Syst.* **40**(10 & 11).
- Goesbet, G. & Letellier, C. [1994] "Global vector field reconstruction by using a multivariate polynomial l_2 approximation on nets," *Phys. Rev.* **E49**(6), 4955–4972.
- Leontaritis, I. J. & Billings, S. A. [1985] "Input-output parametric models for nonlinear systems part II: Stochastic nonlinear systems," *Int. J. Contr.* **41**(2), 329–344.
- Le Sceller, L., Letellier, C. & Goesbet, G. [1996] "Global vector field reconstruction taking into account a control parameter," *Phys. Lett.* **A211**, 211–216.
- Letellier, C., Le Sceller, L., Dutertre, P., Goesbet, G., Fei, Z. & Hudson, J. L. [1995a] "Topological characterization and global vector field reconstruction from an experimental electrochemical system," *J. Phys. Chem.* **99**, 7016–7027.
- Letellier, C., Le Sceller, L., Maréchal, E., Dutertre, P., Maheu, B., Goesbet, G., Fei, Z. & Hudson, J. L. [1995b] "Global vector field reconstruction from a chaotic experimental signal in copper electrodisolution," *Phys. Rev.* **E51**(5), 4262–4266.
- Rico-Martinez, R., Krischer, K., Kevrekidis, I. G., Kube, M. & Hudson, J. L. [1992] "Discrete versus continuous-time nonlinear signal processing of Cu electrodisolution data," *Chem. Eng. Commun.* **118**, 25–48.
- Rosenstein, M. T. [1993] MTRCHAOS version

1.0 ©. available from <http://spanky.triumf.ca/pub/fractals/programs/ibmpc>. Technical report, Dynamical Research, 15 Pecunit Street, Canton, MA 02021-1219, USA. MTR1a@aol.com. also MTRLYAP.

Appendix Retrieving Bifurcation Diagrams by Addition of Multiplicative Noise

This appendix reports a real data situation in which by adding multiplicative noise to a continuous-time model, the original sequence of bifurcations was retrieved. This seems pertinent to the topic discussed in the paper and is presented in what follows.

The reaction here considered is the electrodis-solution of copper in phosphoric acid [Albahadily & Schell, 1988]. It has been observed that, after a Hopf bifurcation, the oscillatory behavior is followed by a period-doubling cascade. Then, a chaotic attractor is observed. The experiments generating the data here used are described in [Letellier *et al.*, 1995a]. A continuous model, constituted by 52 monomials, built on the derivative coordinates has been obtained from a single time series constituted by the time evolution of the current passing through the electrodes. This model was validated

using topological characterization and is very close to the experimental chaotic dynamics [Letellier *et al.*, 1995b].

Surprisingly enough this model can be used to generate time series which correspond to (apparently) unobserved behavior when a multiplicative noise is added to it, as follows

$$\begin{cases} \dot{X} = Y + A_\varepsilon \varepsilon_X(t) \\ \dot{Y} = Z + A_\varepsilon \varepsilon_Y(t) \\ \dot{Z} = F(X, Y, Z) + A_\varepsilon \varepsilon_Z(t), \end{cases} \quad (\text{A.1})$$

where ε_i are three stochastic variables representing some independent Gaussian noise in the range $[-1.0, 1.0]$. Depending on the noise gain A_ε , the model thus settles to different attractors which are observed between the Hopf bifurcation and the chaotic attractor corresponding to the recorded time series. A few examples are displayed in Fig. 4. The amplitude of the noise cannot exceed the critical value of $A_\varepsilon = 0.001615$ beyond which the trajectory is ejected to infinity. The sequence of bifurcations versus the noise amplitude is displayed in Fig. 5.